



**University of
Zurich**^{UZH}

**Zurich Open Repository and
Archive**

University of Zurich
University Library
Strickhofstrasse 39
CH-8057 Zurich
www.zora.uzh.ch

Year: 2014

Site-selective adsorption of phthalocyanine on h-BN/Rh(111) nanomesh

Iannuzzi, Marcella ; Tran, Fabien ; Widmer, Roland ; Dienel, Thomas ; Radican, Kevin ; Ding, Yun ;
Hutter, Jürg ; Gröning, Oliver

DOI: <https://doi.org/10.1039/c4cp01466a>

Posted at the Zurich Open Repository and Archive, University of Zurich

ZORA URL: <https://doi.org/10.5167/uzh-100692>

Journal Article

Supplemental Material

Originally published at:

Iannuzzi, Marcella; Tran, Fabien; Widmer, Roland; Dienel, Thomas; Radican, Kevin; Ding, Yun; Hutter, Jürg; Gröning, Oliver (2014). Site-selective adsorption of phthalocyanine on h-BN/Rh(111) nanomesh. *Physical Chemistry Chemical Physics (PCCP)*, 16(24):12374.

DOI: <https://doi.org/10.1039/c4cp01466a>

I. CALCULATIONS STRUCTURAL AND ELECTRONIC PROPERTIES OF NANOMESH

A. Structural parameters

The modulation of the height of N atoms, of the height of the Rh atoms of the topmost layer of the slab, and of the BN bond length have been calculated along the $[21]$ diagonal of the nanomesh (NM) unit cell. The three different line colors indicate the results for the three tested models, revPBE-D3 (black), PBE-rVV10 (blue), and vdW-DF (red).

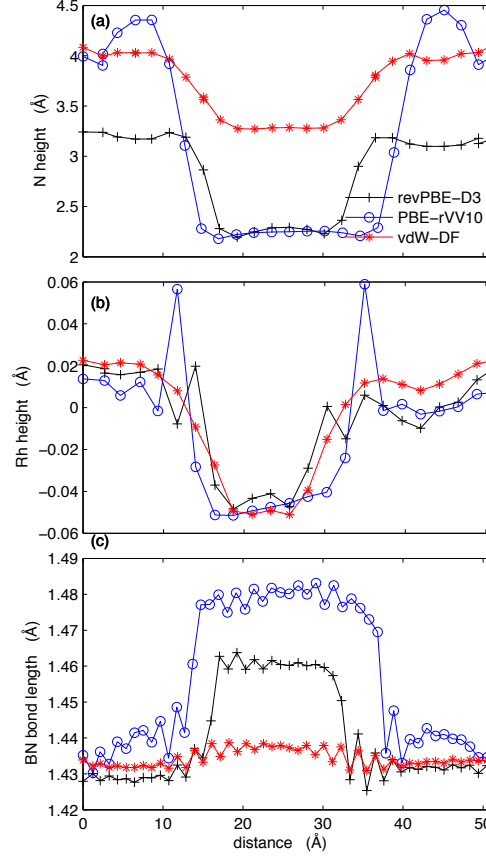


FIG. 1. Height profile over the diagonal crossing the nanomesh unit cell along the $[21]$ direction: (a) N sublattice and (b) Rh atoms of the topmost layer. (c) Modulation of the BN bond length of the atoms laying along the same line. The height of the atoms is measured with respect to the average height of the Rh atoms in the topmost layer.

B. Projected density of states

The (normalized) density of state (DOS) of the h -BN/Rh(111) nanomesh is shown in Figs. 2(a) and 2(b) for the pore and wire regions, respectively. It can be seen that the two functionals lead to DOSs which are very similar, in particular for the pore region. It has already been shown in Refs. 1–3 that the σ -band splitting of about 1 eV measured experimentally⁴ could be well reproduced by the present model of nanomesh (i.e., 13×13 h -BN monolayer on top of 12×12 Rh(111) surface). This shift, coming from the shift between the N- p DOSs of the pore and wire regions can also be observed in the present work.

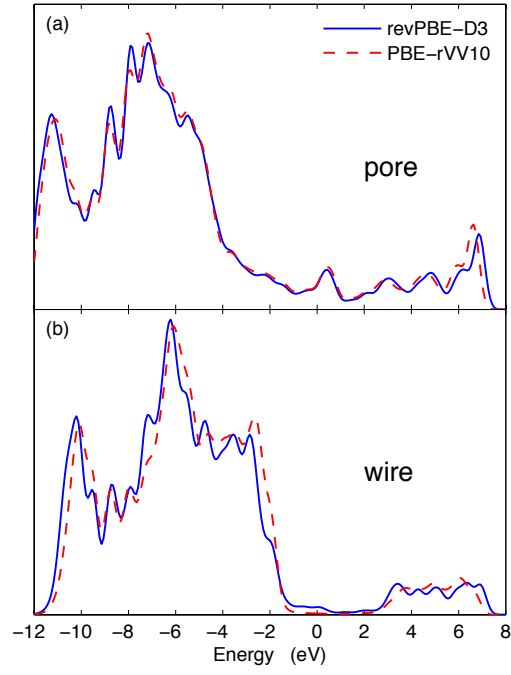


FIG. 2. N- p partial density of states for the N atoms in (a) the pore and (b) the wire regions obtained from the revPBE-D3 and PBE-rVV10 functionals. The curves have been divided by the number of N atoms in their respective regions. The Fermi energy is set at zero.

C. Simulated STM topography

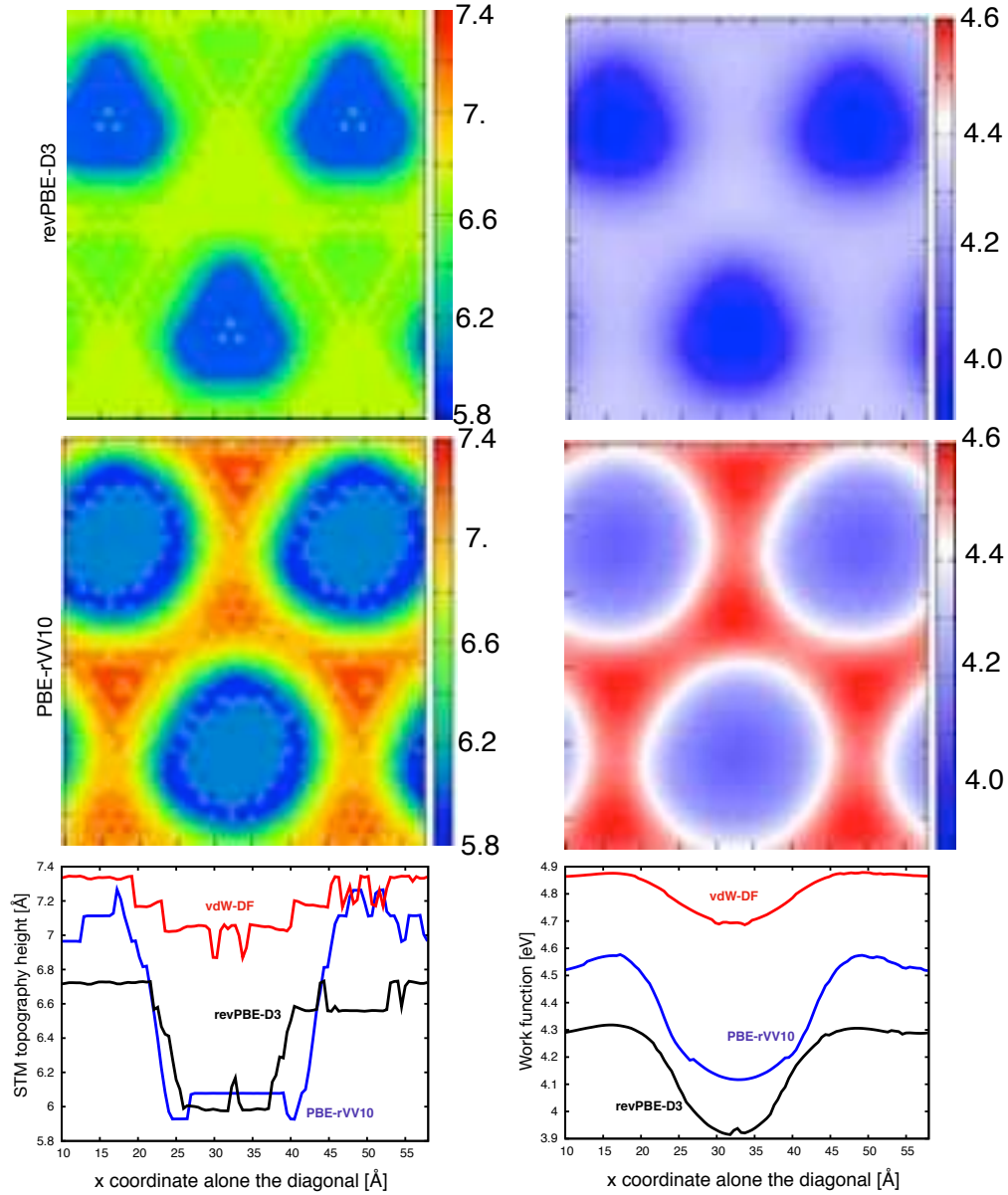


FIG. 3. a) Tersoff-Hamann iso-current surface obtained at a bias potential of -0.5 eV for the revPBE-D3. The axis units are Å. b) Modulation of the local work function calculated at the Tersoff-Hamann iso-current surface displayed in panel a. The values of the work function are in eV. c) Tersoff-Hamann iso-current surface obtained at a bias potential of -0.5 eV for the PBE-rVV10 model. d) Modulation of the local work function calculated at the Tersoff-Hamann iso-current surface displayed in panel c. e) Profiles of the simulated STM topographies (revPBE-D3 black, PBE-rVV10 blue, vdW-DF red) across the unit cell along the [21] direction. f) Profiles of the local workfunction, same direction and color code as in panel e.

II. CALCULATIONS OF H_2PC IN GAS PHASE

The structure of the molecule optimized in gas phase is planar, since all C-C and C-N have sp^2 character. Bond lengths and bond angles do not vary significantly by changing among the three models revPBE-D3, PBE-rVV10, and vdW-DF.

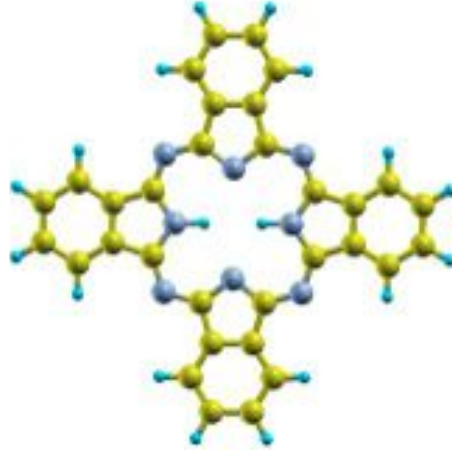


FIG. 4. H_2Pc structure optimized in gas phase: H cyan, C yellow, N grey.

III. CALCULATIONS OF H_2PC ADSORBED ON THE NANOMESH

The calculations have been restricted to the case of H_2Pc , because CuPc requires spin polarized electronic structure optimizations, which makes the convergence slower and increases significantly the computational costs. Every structure optimization involves a simulation cell containing almost 1000 atoms. The system is metallic, which makes the wavefunction optimization slowly converging; typically about 50 iterations of the self consistent cycle are required. The shallow potential energy surface for the adsorption of the molecule makes it difficult to locate the minimum. A typical structure optimization procedure requires the generation of more than 100 configurations.

For all optimized adsorption configurations of H_2Pc on the NM, there are in principle two possible locations of the innermost H atoms. One is with the N-H bonds along the [21] direction, the other is with them perpendicular to the [21] direction. The influence of the H position to the adsorption is first evaluated by structure optimization with the H_2Pc molecule adsorbed to the same position of the nanomesh, but with different N-H orientations. It turned out that the effect of the N-H position is negligible, as the energy difference for the optimized structures is less than 0.4 meV. Thus, all the calculations carried out afterwards are with the N-H bonds perpendicular to the [21] direction.

A. revPBE-D3 adsorption energies

The most stable configuration for the revPBE-D3 model is with H_2Pc centered in the pore. In order to understand

TABLE I. Pc adsorption at the NM: total adsorption energy E_{ads} and the two separated contributions, DFT and dispersion. Distortion energies of NM and Pc, E_{nm} and E_{pc} . Energies are in eV.

Adsorption site	poreA	wire	offA1	offA2
E_{ads}	-3.03 (-2.75) ^a	-2.31	-2.96	-2.93 (-2.93) ^a
E_{DFT}	2.35	2.52	2.72	2.36
E_{dis}	-5.37	-4.83	-5.68	-5.29
E_{nm}	0.077	0.051	0.224	0.053
E_{pc}	0.015	0.017	0.021	0.028

^a The geometry of the nanomesh was kept fixed at the PBE-rVV10 one. The H_2Pc molecule was allowed to relax.

why the preferred adsorption site with revPBE-D3 is the center of the pore while with PBE-rVV10 is off-center, we compare how the DFT and dispersion contributions change. With revPBE-D3, E_{DFT} is 0.37 eV less repulsive for poreA than for offA1, while E_{dis} is only 0.31 eV less attractive. The different contributions almost compensate each other, which makes a 0.07 eV lower adsorption energy for poreA. On the other hand, with PBE-rVV10, the change in the repulsive DFT term between poreA and offA1 is only 0.046 eV in favor of the former, while the gain in dispersion of offA1 is of 0.227 eV. This can be explained with the fact that at the center of the larger PBE-rVV10

NM pore, the molecule minimize the interaction with the atoms of the rim, and all its atoms are equally distant from the closest BN pairs. Moving the molecule towards the rim there is enough space to let the attractive dispersion interaction to increase, between one lobe of the molecule and the rim, still keeping the repulsive term small. With the revPBE-D3, the molecule is almost as large as the NM pore, and already when centered in the pore, some of its atoms are already quite close to the rim. Pushing the molecule further towards the rim brings one lobe almost beyond the it, thus increasing the attraction term between C atoms and BN pairs, but also inducing an equal increase of the repulsive contribution. In order to confirm the implications of the pore shape, H₂Pc has been optimized with revPBE-D3 on the fixed NM geometry as obtained with PBE-rVV10. Similarly, we have optimized H₂Pc with PBE-rVV10 on the fixed revPBE-D3 NM. It turns out that with the PBE-rVV10 NM shape the off center adsorption is always favorite, irrespective of the functional used to calculate the interaction.

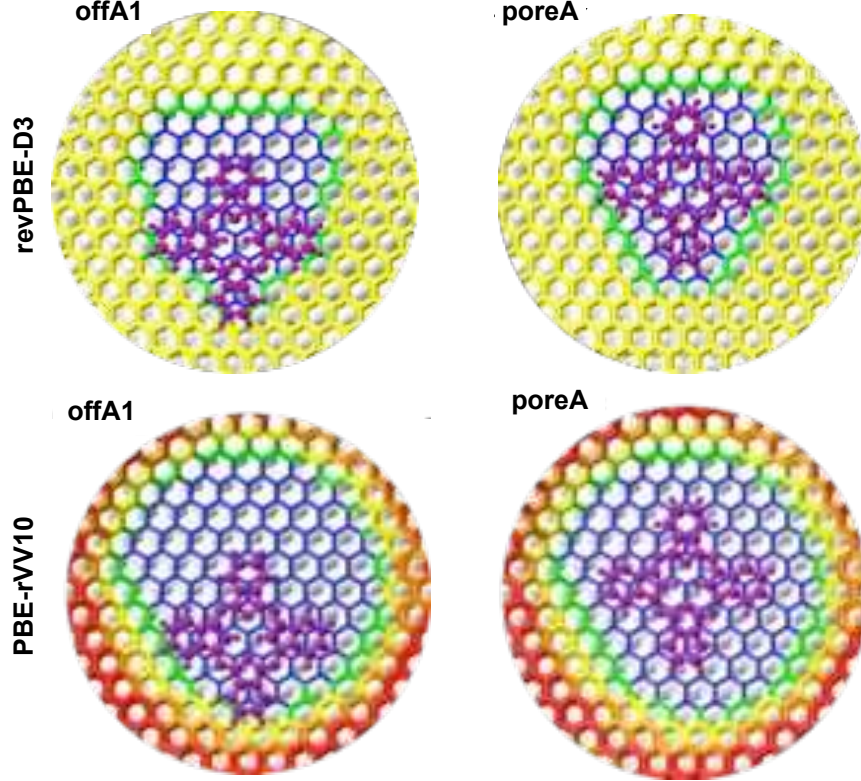


FIG. 5. Top view of Pc adsorbed on the NM in poreA and offA1 configurations as obtained with the revPBE-D3 functional (top) and with the PBE-rVV10 functional (bottom). The atoms of the *h*-BN lattice are colored according to their height over the Rh surface: Blue $d_z < 2.4$ (pore), yellow $2.4 < d_z < 3.7$, red $d_z > 3.7$. The atoms of H₂Pc are all magenta.

With the vdW-DF functional the adsorption energy of H₂Pc in the does not change significantly depending on the specific site. It is always about 3.06 eV. Due to the choice of the functional and the less corrugated *h*-BN layer, the distance between BN and molecule is larger and does not change significantly by moving the molecule over the pore. Hence, the two terms of the interaction energy change also little.

B. Electronic structure of adsorbed H₂Pc

The charge density difference $\Delta\rho(\mathbf{r})$ is calculated as

$$\Delta\rho(\mathbf{r}) = \rho_{\text{pc/NM}}(\mathbf{r}) - \rho_{\text{pc}}(\mathbf{r}) - \rho_{\text{NM}}(\mathbf{r}), \quad (1)$$

where $\rho_{\text{pc}}(\mathbf{r})$ and $\rho_{\text{NM}}(\mathbf{r})$ are the charge densities of the two subsystems taken alone, but in the same geometry of the complex. These volumetric data structures represent the changes in the electronic charge distribution due to the interaction between molecule and substrate. The rather small $\Delta\rho(\mathbf{r})$ computed for all pc/NM configurations confirm that no chemical bonding is formed. However, some polarization effects are present, as it can be observed in the

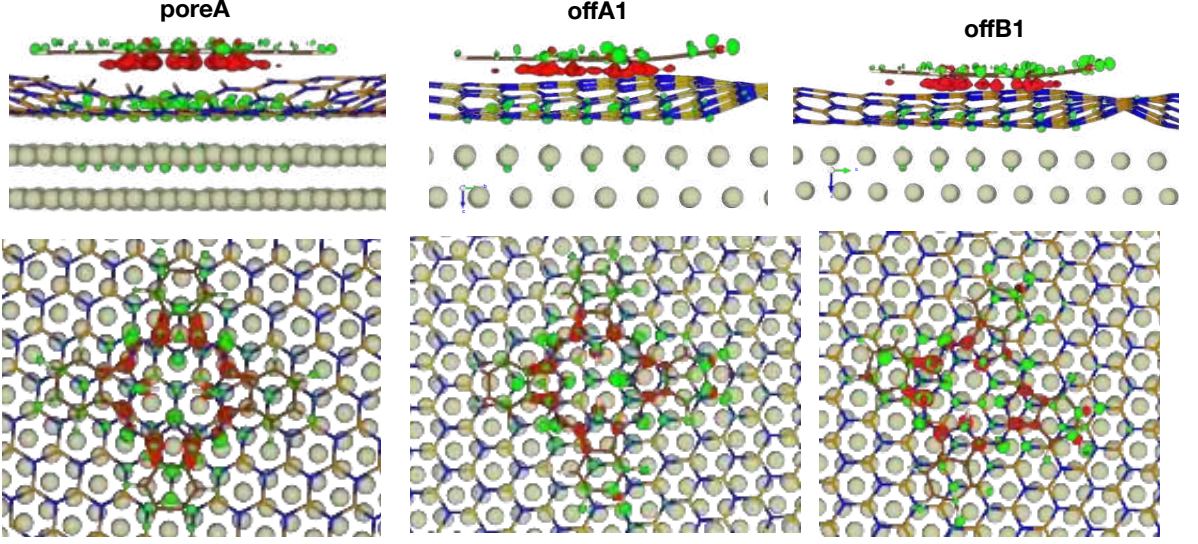


FIG. 6. Density difference plots: side view (top) and top view (bottom) of the $\Delta\rho$ isosurface at $+0.007 \text{ el}/\text{\AA}^3$ (red) and $-0.007 \text{ el}/\text{\AA}^3$ (green) calculated for three optimized structures, poreA, offA1, and offB1. The Pc molecule and the h -BN layer are represented by lines along the bonds. C are brown, H white, N blue and B orange. The Rh substrate is represented by grey balls. Each panel displays only a portion of the NM unit cell.

plots of $\Delta\rho(\mathbf{r})$ isosurfaces displayed in figure 6 for three configurations, poreA, offA1 and offB1. The red isosurface corresponds to accumulation of charge, and it is mainly located in the area below the pyrrole-like subunits, indicating polarization of the molecular charge towards the substrate. The corresponding charge depletion is illustrated by the green isosurface and it is localized close to atomic centers of the molecule (mainly H and N) and at some N and B of the NM pore underneath the molecule. The electron distribution at the metal, instead, is barely affected by the presence of the molecule.

The dipole moment of the H_2Pc molecule in gas phase and adsorbed on the surface has been calculated using the method of the maximally localized Wannier function (MLWF)². Once the localization procedure has converged, the MLWF are associated either to the molecule or to the substrate. The center of the MLWF, i.e. the Wannier center, represents the position of the localized electron pairs, charge -2. The atomic positions are instead the location of the positive core charges, i.e. +5 for N, +4 for C, and +1 for H. The dipole moment is then obtained from the sum over all the particles, ionic cores and Wannier centers, of the product of the position vector times the corresponding charge

$$\boldsymbol{\mu} = \sum_{I=1}^{N_{\text{atom}}} \mathbf{R}_I q_I - 2 \sum_{x=1}^{N_{\text{wc}}} \mathbf{R}_x \quad (2)$$

In gas phase, all the three Cartesian components of the dipole are null. The interaction with the substrate, instead, induces a molecular dipole, with the largest component in the direction perpendicular to the surface, μ_z .

TABLE II. Dipole moment components and norm in Debye

Adsorption site	poreA	wire	offA1	offB1
μ_x	-1.526	-2.151	.944	0.044
μ_y [21]	-.271	-1.039	1.339	3.340
μ_z	5.105	1.298	5.365	5.387
μ	5.336	2.719	5.610	6.338

We have computed the projected density of states (PDOS) for H_2Pc in gas phase and adsorbed in the offA1 configuration. In figure 7 (a) and (b), the black curves are the PDOS on C atoms and N atoms, respectively, where the energies are reported with respect to the center of the homo-lumo gap. The isosurfaces corresponding to the wavefunctions of the homo-1, homo, lumo and lumo+1 states are displayed in panel (c). The same PDOS computed for the molecule adsorbed in the offA1 configuration are reported in red. In this case the energies are given with respect to the Fermi energy. It is noticed that the lumo of H_2Pc is almost aligned with the Fermi energy of the

complex. Otherwise, the structure of the molecular orbitals seems not to be significantly perturbed by the interaction with the substrate.

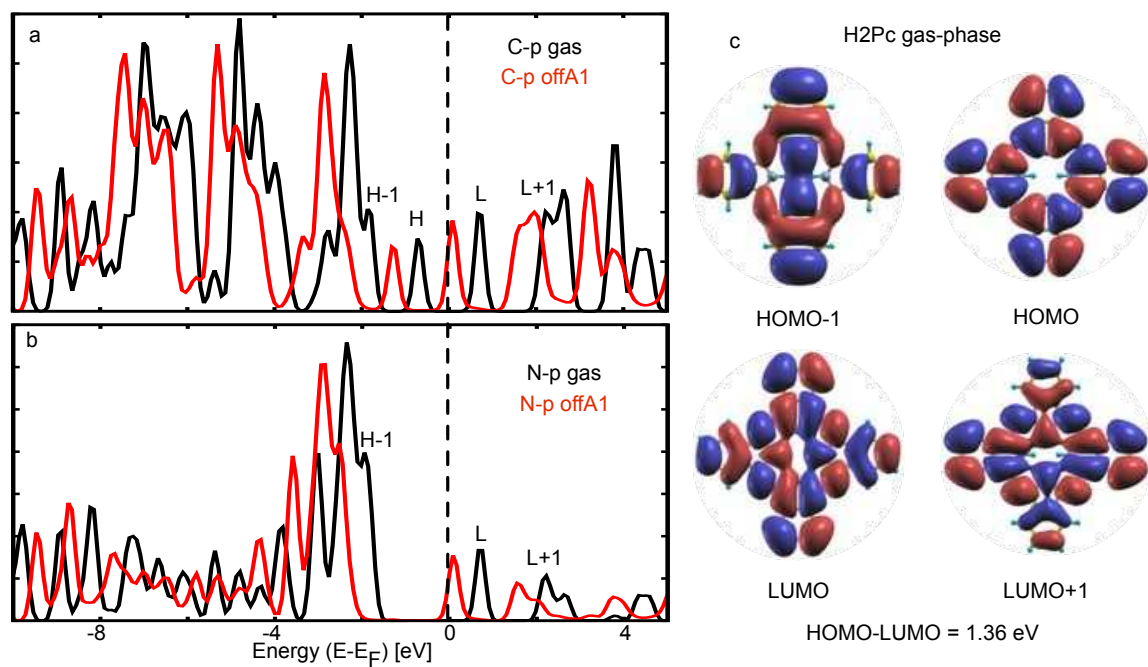


FIG. 7. a) and b) projected density of states on C and N atoms of H₂Pc, respectively. The black curve is the PDOS computed for the molecule optimized in gas phase, the red curve for the molecule adsorbed in the offA1 configuration.

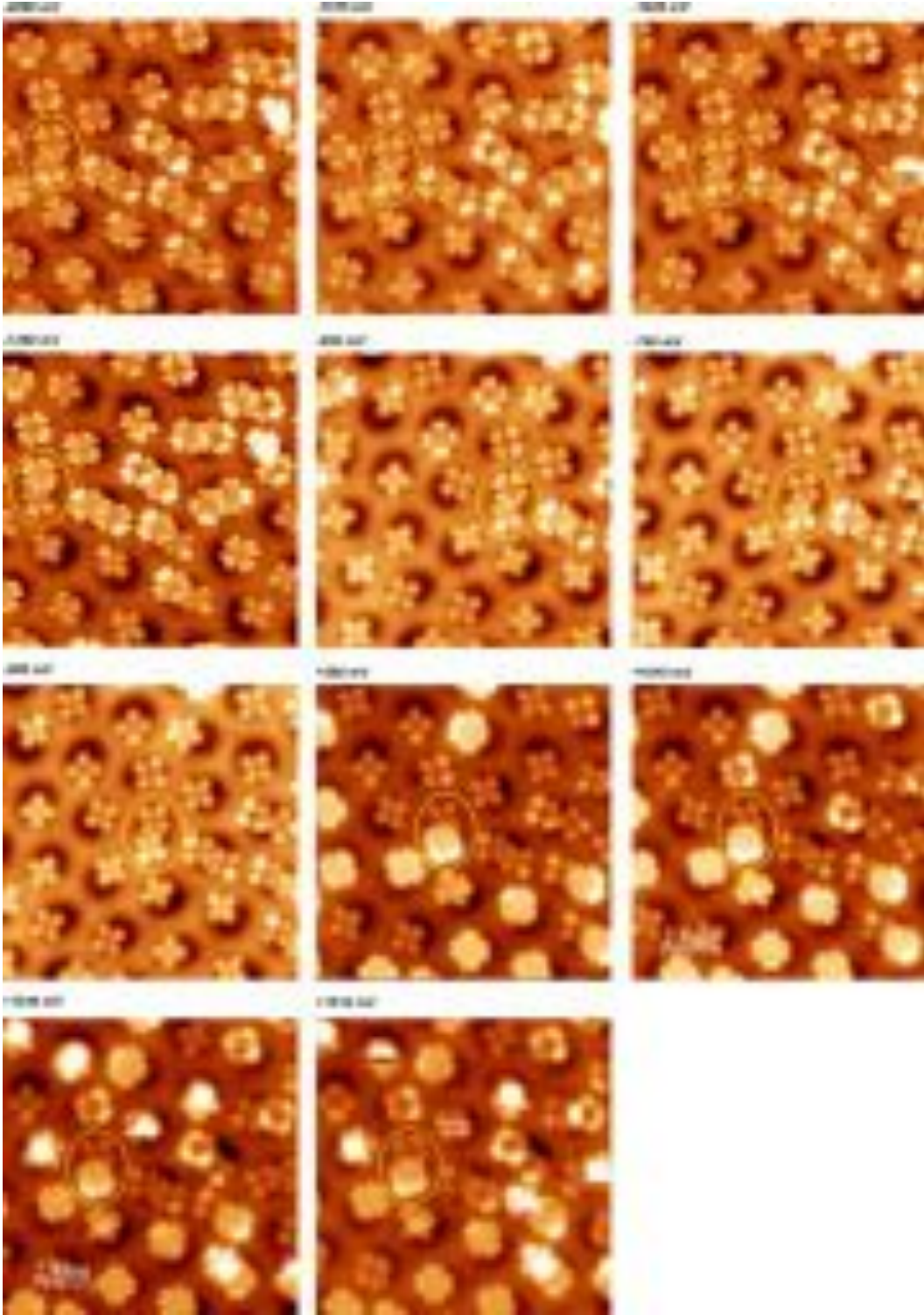


FIG. 8. Sequence of constant current STM images at different biases showing the energy variations in the HOMO-LUMO positions of H_2PC on the $h\text{-BN/Rh(111)}$ NM. All images have been measured at 26 pA set point current. The yellow circle denotes the same position in all images.

C. Mobility within the pore

At higher temperature the molecules cannot be imaged stably anymore, but that they are pushed around in the pore during the STM scanning. The “double cross” configuration seen the figure originates from the bi-stable position of the molecule in the pore and not from two molecules sitting in the same pore. This later situation is realized at higher molecule coverage as can be seen in the figure 8, where the two molecules in the pore are well resolved. Depending on the tip condition and tunneling parameters the images at 77 K can become very blurred due to the mobility of the molecules in the pore. Despite the mobility the molecules are not pushed out of the pores.

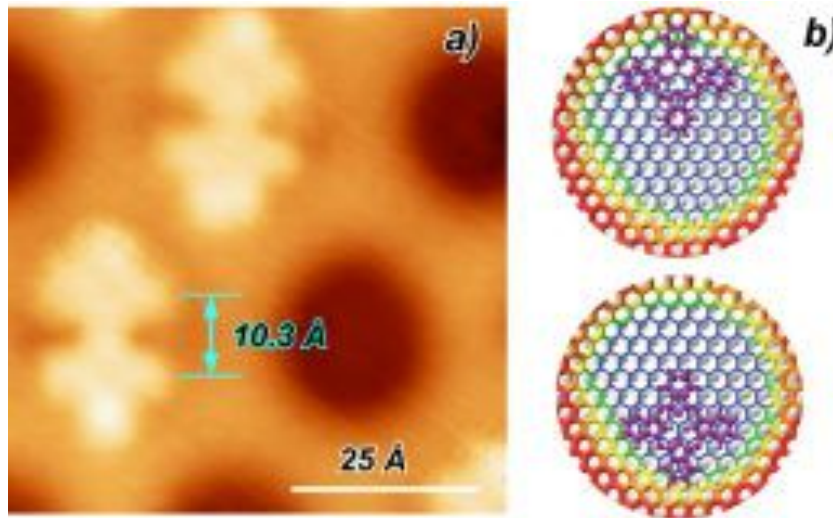


FIG. 9. a) Constant current STM image of CuPc on the *h*-BN/Rh(111) NM measured at 77 K where a single molecule per pore is imaged switching between two off-center positions. The image is rotated 45° with regard to the scan direction, i.e. the direction of the molecule displacement is not in the direction of the scan. b) DFT minimum energy configurations of H₂Pc on opposite off-center positions.

¹ R. Laskowski, P. Blaha, T. Gallauner, and K. Schwarz, Phys Rev Lett **98**, 106802 (2007).

² R. Laskowski and P. Blaha, J. Phys.: Condens. Matter **20**, 064207 (2008).

³ R. Laskowski and P. Blaha, Phys. Rev. B **81**, 075418 (2010).

⁴ M. Corso, W. Auwärter, M. Muntwiler, A. Tamai, T. Greber, and J. Osterwalder, Science **303**, 217 (2004).